

# Rational design of self-assembly pathways for complex multicomponent structures

William M. Jacobs,<sup>1</sup> Aleks Reinhardt,<sup>1</sup> and Daan Frenkel<sup>1</sup>

*Department of Chemistry, University of Cambridge, Lensfield Road, Cambridge CB2 1EW, United Kingdom*

(Dated: 3 April 2015)

The field of complex self-assembly is moving toward the design of multi-particle structures consisting of thousands of distinct building blocks. To exploit the potential benefits of structures with such ‘addressable complexity,’ we need to understand the factors that optimize the yield and the kinetics of self-assembly. Here we use a simple theoretical method to explain the key features responsible for the unexpected success of DNA-brick experiments, which are currently the only demonstration of reliable self-assembly with such a large number of components. Simulations confirm that our theory accurately predicts the narrow temperature window in which error-free assembly can occur. Even more strikingly, our theory predicts that correct assembly of the complete structure may require a time-dependent experimental protocol. Furthermore, we predict that low coordination numbers result in non-classical nucleation behavior, which we find to be essential for achieving optimal nucleation kinetics under mild growth conditions. We also show that, rather surprisingly, the use of heterogeneous bond energies improves the nucleation kinetics and in fact appears to be necessary for assembling certain intricate three-dimensional structures. This observation makes it possible to sculpt nucleation pathways by tuning the distribution of interaction strengths. These insights not only suggest how to improve the design of structures based on DNA bricks, but also point the way toward the creation of a much wider class of chemical or colloidal structures with addressable complexity.

## SIGNIFICANCE STATEMENT:

Recent experiments have demonstrated that complex, three-dimensional nanostructures can be self-assembled out of thousands of short strands of pre-programmed DNA. However, the mechanism by which robust self-assembly occurs is poorly understood, and the same feat has not yet been achieved using any other molecular building block. Using a novel theory of ‘addressable’ self-assembly, we explain how the design of the target structure and the choice of inter-particle interactions determine the self-assembly pathway, and, for the first time, predict that a time-dependent protocol, rather than merely a carefully tuned set of conditions, may be necessary to optimize the yield. With an understanding of these design principles, it should be possible to engineer addressable nanostructures using a much wider array of materials.

Recent experiments with short pieces of single-stranded DNA<sup>1,2</sup> have shown that it is possible to assemble well-defined molecular superstructures from a single solution with more than merely a handful of distinct building blocks. These experiments use complementary DNA sequences to encode an addressable structure<sup>3</sup> in which each distinct single-stranded ‘brick’ belongs in a specific location within the target assembly. A remarkable feature of these experiments is that even without careful control of the subunit stoichiometry or optimization of the DNA sequences, a large number of two- and three-dimensional designed structures with thousands of subunits assemble reliably.<sup>1,2,4,5</sup> The success of this approach is astounding given the many ways in which the assembly of an addressable structure could potentially go wrong.<sup>6-8</sup>

Any attempt to optimize the assembly yield or to create even more complex structures should be based on a better understanding of the mechanism by which DNA bricks manage to self-assemble robustly. The existence of a sizable nucleation barrier, as originally proposed in Refs. 1 and 2, would remedy two possible sources of error that were previously thought to limit the successful assembly of multicomponent nanostructures: the depletion of free monomers and the uncontrolled aggregation of partially formed structures. Slowing the rate of nu-

cleation would suppress competition among multiple nucleation sites for available monomers and give the complete structure a chance to assemble before encountering other partial structures. Recent simulations of a simplified model of a three-dimensional addressable structure have provided evidence of a free-energy barrier for nucleation,<sup>9</sup> suggesting that the ability to control this barrier should enable the assembly of a wide range of complex nanostructures. We therefore need to be able to predict how such a barrier depends on the design of the target structure and on the choice of DNA sequences. Until now, however, there have been no reliable techniques to predict the existence, let alone the magnitude, of a nucleation barrier for self-assembly in a mixture of complementary DNA bricks.

Here we show that the assembly of three-dimensional DNA-brick nanostructures is indeed a nucleated process, but only in a narrow range of temperatures. The nucleation barrier in these systems is determined entirely by the topology of the designed interactions that stabilize the target structure. Controllable nucleation is therefore a general feature of addressable structures that can be tuned through the rational choice of designed interactions. We find that the reliable self-assembly of three-dimensional DNA bricks is a direct consequence of their unusual nucleation behavior, which is not accounted for

by existing theories that work for classical examples of self-assembly, such as crystal nucleation. We are thus able to provide a rational basis for the rather unconventional protocol used in the recent DNA-brick experiments by showing that they exploit a narrow window of opportunity where robust multicomponent self-assembly can take place.

## STRUCTURE CONNECTIVITY DETERMINES ASSEMBLY

In constructing a model for the self-assembly of addressable structures, we note that the designed interactions should be much stronger than any attractive interactions between subunits that are not adjacent in a correctly assembled structure. The designed interactions that stabilize the target structure can be described by a connectivity graph,  $G$ , in which each vertex represents a distinct subunit and each edge indicates a correct bond. This graph allows us to describe the connectivity of the structure without specifying the geometric details and spatial organization of the building blocks. For structures constructed from DNA bricks, the edges of  $G$  indicate the hybridization of DNA strands with complementary sequences that are adjacent in the target structure. An example three-dimensional DNA-brick structure is shown along with its connectivity graph in Figures 1a and 1b.

In an ideal solution with exclusively designed interactions, the subunits assemble into clusters in which all allowed bonds are encoded in the connectivity graph of the target structure. In order to compute the free-energy difference between on-pathway clusters of a particular size and the unbonded single-stranded bricks, we must consider all the ways in which a correctly bonded cluster with a given number of monomers can be assembled. These clusters can be described by the distinct ‘fragments’ of the target structure, which correspond to connected subgraphs of the connectivity graph. In a dilute solution with strong designed interactions, the numbers of edges and vertices are the primary factors determining the stability of a particular fragment. We therefore identify all possible assembly intermediates by grouping fragments into sets with the same number of edges and vertices and counting the total number of fragments in each set. This calculation yields the ‘density of states’ of fragments of the target structure, which is an intrinsic property of the connectivity graph. We combine the density of states with information about the subunit geometries, monomer concentrations and designed bond strengths to compute the free energies of the on-pathway clusters. We can also estimate the equilibrium probability of forming competing off-pathway structures, the overwhelming majority of which arise from undesired incidental interactions between subunits. For further discussion of the theory, please see the Supplementary Information Sec. S1 and Ref. 10.

This theoretical approach is powerful because it can

predict the free-energy landscape as a function of the degree of assembly between the monomers and the target structure. Furthermore, the predicted landscape captures the precise topology of the target structure, which is essential for understanding the assembly of addressable, finite-sized structures. In the case of DNA-brick structures, we can assign DNA hybridization free energies to the edges of the target connectivity graph in order to determine the temperature dependence of the free-energy landscape; for example, Figure 1d shows the free-energy profile of the 86-strand DNA-brick structure with random DNA sequences at three temperatures. Our theoretical approach allows us to calculate the nucleation barrier,  $\Delta F^\ddagger$ , by examining the free energies of clusters corresponding to fragments with exactly  $V$  vertices. The critical number of strands required for nucleation is  $V^\ddagger$ : transient clusters with fewer than  $V^\ddagger$  strands are more likely to dissociate than to continue incorporating additional strands. The presence of a substantial nucleation barrier therefore inhibits the proliferation of large, partially assembled fragments that stick together to form non-target aggregates.

## ASSEMBLY REQUIRES A TIME-DEPENDENT PROTOCOL

Over a significant range of temperatures, we find that the free-energy profiles of DNA-brick structures exhibit both a nucleation barrier and a thermodynamically stable intermediate structure. The nucleation barrier is associated with the minimum number of subunits that must be assembled in order to complete one or more *cycles*, i.e. closed loops of stabilizing bonds in a fragment. For example, the critical number of monomers in the example structure at 319 K,  $V^\ddagger = 8$ , is one fewer than the nine subunits required to form a bicyclic fragment of the target structure. Under the conditions where nucleation is rate controlling, the minimum free-energy structure is *not* the complete 86-particle target structure, but rather a structure with only  $V \simeq 65$  particles. This incomplete structure is favored by entropy, since it can be realized in many more ways than the unique target structure. Hence, the temperature where nucleation is rate controlling is higher than the temperature where the target structure is the most stable cluster. The existence of thermodynamically stable intermediates is a typical feature of DNA-brick structures and of complex addressable, finite-sized structures in general.<sup>11</sup>

This behavior is not compatible with classical nucleation theory (CNT), which predicts that, beyond the nucleation barrier, large clusters are always more stable than smaller clusters. As a consequence, in ‘classical’ nucleation scenarios such as crystallization, there is a sharp boundary in temperature and concentration at which the largest-possible ordered structure, rather than the monomeric state, becomes thermodynamically stable. Typically, a simple fluid must be supersaturated

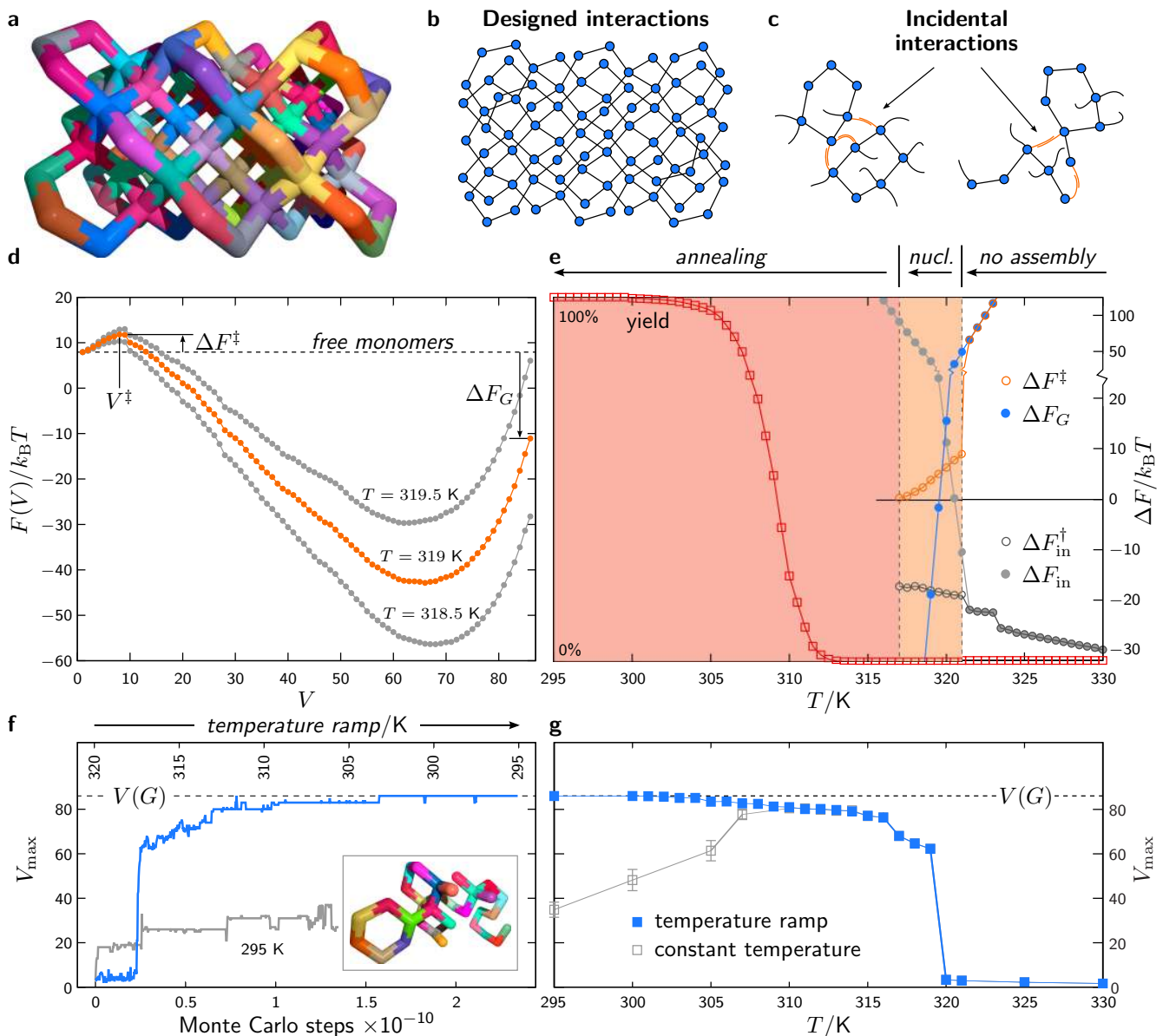


FIG. 1. Controlled nucleation is essential for robust self-assembly. (a) An example 86-strand DNA-brick structure and (b) its associated connectivity graph. (c) Incidental interactions between dangling ends, shown in orange, lead to incorrect associations between fragments. (d) Free energies of clusters of  $V$  subunits with randomly chosen DNA sequences in units of  $k_B T$ , where  $k_B$  is the Boltzmann constant and  $T$  is the absolute temperature. The nucleation barrier,  $\Delta F^\ddagger$ , and the target structure stability,  $\Delta F_G$ , are strongly temperature-dependent. (e) The equilibrium yield with exclusively designed interactions and the nucleation barrier as a function of temperature. Also shown are the target structure stability and the free-energy difference between all off-pathway and on-pathway intermediates, in the presence,  $\Delta F_{in}^\ddagger$ , and absence,  $\Delta F_{in}$ , of a nucleation barrier. The nucleation window is shown in orange. (f) Representative lattice Monte Carlo simulation trajectories with (blue) and without (gray) a temperature ramp; a typical malformed structure is shown in the inset. (g) The size of the largest correctly bonded stable cluster in lattice Monte Carlo simulations using a temperature ramp (blue) and in constant-temperature simulations initialized from free monomers in solution (gray).

well beyond this boundary in order to reduce the nucleation barrier, which arises due to the competition between the free-energy penalty of forming a solid-liquid interface and the increased stability due to the growth of an ordered structure.<sup>12–14</sup> Yet in the case of addressable self-assembly, and DNA bricks in particular, a nucleation

barrier for the formation of a stable partial structure may exist even when the target structure is unstable relative to the free monomers.

An experiment to assemble such a structure requires a *protocol*: first nucleation at a relatively high temperature, and then further cooling to complete the forma-

tion of the target structure.<sup>15</sup> This behavior can be seen in Figure 1e, where we identify a narrow temperature window in which there is a significant yet surmountable nucleation barrier. Unlike CNT, the nucleation barrier does not diverge as the temperature is increased. Instead, there is a well-defined temperature above which all clusters have a higher free energy than the free monomers. As the temperature is lowered further, the nucleation barrier disappears entirely before the equilibrium yield, defined as the fraction of all clusters that are correctly assembled as the complete target structure, increases measurably above zero. The equilibrium yield tends to 100% at low temperatures, since we have thus far assumed that only designed interactions are possible. Therefore, because of the presence of stable intermediate structures, it is typically impossible to assemble the target structure completely at any temperature where nucleation is rate controlling.

In order to examine the importance of a nucleation barrier for preventing misassembly, we estimate the free-energy difference between off-pathway aggregates and all on-pathway intermediates,  $\Delta F_{\text{in}}$ , by calculating the probability of incidental interactions between partially assembled structures.<sup>10</sup> From the connectivity graph of the example DNA-brick structure, we can calculate the total free energy of aggregated clusters by considering all the ways that partially assembled structures can interact via the dangling ends of the single-stranded bricks, as shown in Figure 1c. We also estimate this free-energy difference in the case of slow nucleation,  $\Delta F_{\text{in}}^\ddagger$ , by only allowing one of the interacting clusters in a misassembled intermediate to have  $V > V^\ddagger$ .

The above analysis supports our claim that a substantial nucleation barrier is essential for accurate self-assembly. Our calculations show that even with very weak incidental interactions, incorrect bonding between the multiple dangling ends of large partial structures prevents error-free assembly at equilibrium, since  $\Delta F_{\text{in}} > 0$ . The presence of a nucleation barrier slows the approach to equilibrium, maintaining the viability of the correctly assembled clusters.

These theoretical predictions are confirmed by extensive Monte Carlo simulations of the structure shown in Figure 1a. In these simulations, the DNA bricks are modeled as rigid particles that move on a cubic lattice, but otherwise the sequence complementarity and the hybridization free energies of the experimental system are preserved.<sup>9</sup> Using realistic dynamics,<sup>16</sup> we simulate the assembly of the target structure using a single copy of each monomer. In Figure 1f, we compare a representative trajectory from a simulation using a linear temperature ramp with a trajectory from a constant-temperature simulation starting from free monomers in solution. We also report the largest stable cluster size averaged over many such trajectories in Figure 1g. Nucleation first occurs within the predicted nucleation window where  $\Delta F^\ddagger \simeq 8 k_B T$ . At 319 K, the size of the largest stable cluster coincides precisely with the pre-

dicted average cluster size at the free-energy minimum in Figure 1d.<sup>17</sup> Intermediate structures assembled via a temperature ramp continue to grow at lower temperatures, while clusters formed directly from a solution of free monomers become arrested in conformations that are incompatible with further growth (Figure 1f, *inset*). In agreement with our theoretical predictions, the simulation results demonstrate that a time-dependent protocol is essential for correctly assembling a complete DNA-brick structure.

## COORDINATION NUMBER CONTROLS THE NUCLEATION BARRIER

In the modular assemblies reported in Ref. 2, the maximum coordination number of bricks in the interior of the structure is four. However, one can envisage other building blocks, such as functionalized molecular constructs or nano-colloids, that have a different coordination number. To investigate the effect of the coordination number on the nucleation barrier, we compare the free-energy profile of a 48-strand DNA-brick structure with those of two higher-coordinated structures (Figure 2a): a simple cubic structure with coordination number  $q_c = 6$  and a close-packed structure with  $q_c = 12$ . (For a discussion of two-dimensional structures, see Sec. S4.) In Figure 2b, we show the free-energy profiles at 50% yield assuming identical bond energies within each structure.

One striking difference between the  $q_c = 4$  structure and the higher-coordinated examples is the stability of the target at 50% yield. In the DNA-brick structure, the target structure coexists in nearly equal populations with a partial structure that is missing a single cycle. In the structures with higher coordination numbers, however, the target has the same free energy as the free monomers at 50% yield. Intermediate structures are therefore globally unstable at all temperatures, as predicted by CNT.

A second point of distinction among these structures lies in the relative stability of intermediate cluster sizes. Whereas the DNA-brick structure assembles by completing individual cycles, the cubic structure grows by adding one face at a time to an expanding cuboid.<sup>18</sup> With  $q_c = 12$ , the greater diversity of fragments with the same number of vertices smooths out the free-energy profile near the top of the nucleation barrier. The fitted black line in Figure 2b shows that the assembly of this structure does in fact obey CNT (see Sec. S2).

The differences among these free-energy profiles originate from the topologies of the connectivity graphs of the example structures. The most important determinant of the nucleation behavior is simply the number of vertices required to complete each additional cycle in the target connectivity graph, which is controlled by the maximum coordination number of the subunits.<sup>19</sup> Our findings imply that controlled self-assembly of three-dimensional addressable structures is unlikely to be achieved straightforwardly using subunits with coordination numbers higher

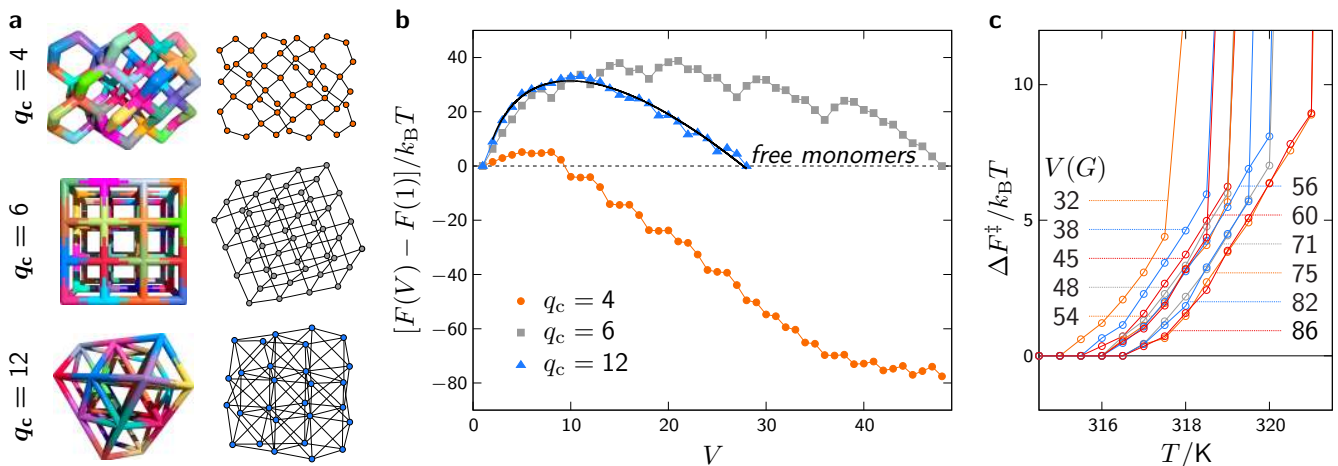


FIG. 2. Dependence of the nucleation barrier on the coordination number of the target structure. (a) Example structures with tetrahedral coordination ( $q_c = 4$ ), octahedral coordination ( $q_c = 6$ ) and close-packed coordination ( $q_c = 12$ ), along with their associated connectivity graphs. (b) Free-energy profiles of these three structures at 50% yield assuming identical bond energies within each structure. The black line shows the fit of classical nucleation theory to the nucleation barrier of the  $q_c = 12$  structure. (c) The dependence of the nucleation barrier on the total number of strands,  $V(G)$ , in DNA-brick structures with randomly chosen DNA sequences. The nucleation temperature does not increase monotonically with  $V(G)$  in these roughly cuboidal structures since surface effects are considerable.

than four. In higher-coordinated structures, which are well described by CNT, it would be necessary to go to high supersaturation in order to find a surmountable nucleation barrier; however, such an approach is likely to fail due to kinetic trapping.<sup>20</sup> Yet in DNA-brick structures, the nucleation barrier is surmountable at low supersaturation and is relatively insensitive to the size of the target structure (Figure 2c). The reliable self-assembly of large DNA-brick structures is thus a direct consequence of the small number of bonds made by each brick.

### HETEROGENEOUS BOND ENERGIES IMPROVE KINETICS

Recent publications have argued that equal bond energies should enhance the stability of the designed structure<sup>21</sup> and reduce errors during growth.<sup>22</sup> By contrast, we find that the kinetics of DNA-brick assembly are actually worse if one selects DNA sequences that minimize the variance in the bond energies. Our observation is consistent with the successful use of random DNA sequences in the original experiments with DNA bricks.<sup>1,2</sup> Here again, the nucleation behavior is responsible for this unexpected result.

To demonstrate the difference between random DNA sequences and sequences chosen to yield monodisperse bond energies, we consider the relatively simple non-convex DNA-brick structure shown in Figure 3a. This 74-brick structure, constructed by removing the interior strands and two faces from a cuboidal structure, assembles roughly face-by-face when using random DNA sequences. The relevant nucleation barrier, as predicted

theoretically in Figure 3b and confirmed with Monte Carlo simulations in Figure 3c, is the completion of the third face. With monodisperse bond energies and an equivalent mean interaction strength, a much larger nucleation barrier appears before the first face forms. Attempts to reduce this nucleation barrier by increasing the mean bond energy result in kinetic trapping and arrested growth. Despite promising fluctuations in the largest cluster size in the simulation trajectory with monodisperse energies, multiple competing nuclei appear, and the largest cluster remains poorly configured for further assembly (Figure 3c, *inset*).

The use of sequences with a broad distribution of hybridization free energies results in a more suitable nucleation barrier because such a distribution selectively stabilizes small and floppy intermediate structures. This is a statistical effect: since there are far fewer ways of constructing a maximally connected fragment with a given number of monomers, the chance that randomly assigned sequences concentrate the strongest bonds in a compact fragment is vanishingly small in a large structure. As a result, the dominant nucleation pathways no longer need to follow the maximally connected fragments. The use of a broad distribution of bond energies therefore tends to reduce nucleation barriers, since unstable fragments near the top of a barrier contain fewer cycles and are thus affected more significantly by the variance in the bond-energy distribution.

### DESIGN PRINCIPLES FOR (DNA) NANOSTRUCTURES

The insights provided by our predictive theory allow us to understand the general principles underlying the

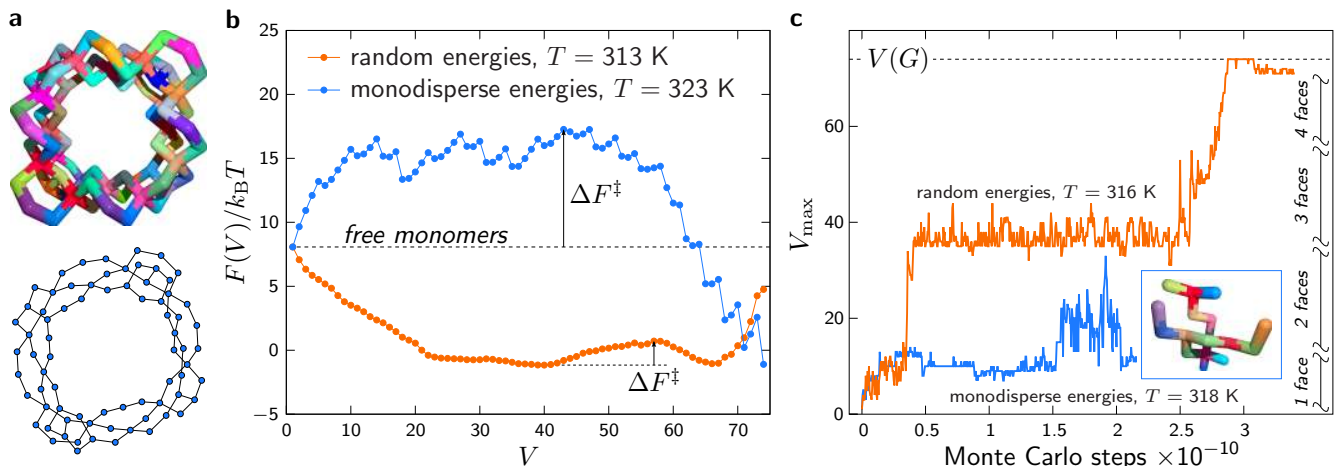


FIG. 3. Random DNA sequences can improve the kinetics of self-assembly. (a) A non-convex, 74-strand DNA-brick structure and its associated connectivity graph. (b) Free-energy profiles and effective nucleation barriers,  $\Delta F^\ddagger$ , with both random and monodisperse designed interaction strengths. The temperatures are chosen such that the mean hybridization free energies of these two distributions are equal. (c) Representative lattice Monte Carlo simulation trajectories with heterogeneous and monodisperse bond energies. Correct assembly proceeds by assembling one face of the structure at a time, as shown on the right. The temperature of the monodisperse system must be lowered to achieve nucleation, but the largest cluster quickly becomes kinetically trapped (*inset*).

unexpected success of DNA-brick self-assembly. Slow, controlled nucleation at low supersaturation is achieved for large structures since each brick can only make a small number of designed connections. Because of an appreciable nucleation barrier that appears in a narrow temperature window, monomer depletion does not pose a significant problem for one-pot assembly. Surprisingly, complex structures with randomly selected complementary DNA sequences experience enhanced nucleation, making larger intermediate structures kinetically accessible at higher temperatures.

The use of a temperature ramp plays a more crucial role than previously thought. Cooling the DNA-brick solution slowly is not just a convenient way of locating good assembly conditions, as in the case of conventional crystals; rather, it is an essential non-equilibrium protocol for achieving error-free assembly of finite-sized structures. The explanation of slow nucleation and fast growth that was originally proposed in Refs. 1 and 2 is therefore incomplete: fast growth allows the DNA bricks to assemble into a stable, on-pathway intermediate that must be annealed at lower temperatures to complete the target structure. For nucleation to be rate controlling, the monomers must diffuse sufficiently rapidly for the solution of precritical clusters to reach equilibrium. With this assumption, our results suggest that the growth of supercritical clusters proceeds by monomer addition and that, as a result, incorrect assembly is rare. However, successful assembly also relies on the slow diffusion of large intermediates, whose rate of diffusion changes approximately inversely with the cluster radius.<sup>23</sup> Remaining out of equilibrium throughout the assembly protocol is necessary in order to avoid the aggregation of these partial structures, which we predict to be the globally

favored thermodynamic state.

Our approach also suggests how to improve the design of DNA-brick nanostructures beyond the random selection of uniformly distributed DNA sequences. For a given target structure, it is easy to tune the nucleation barrier by adjusting the statistical distribution of bond energies. Complementary DNA sequences can then be assigned to the structure in order to achieve the desired distribution of hybridization free energies. Furthermore, with an understanding of the origin of the nucleation barrier in a particular structure, it is possible to optimize the annealing protocol rationally in order to increase the yield of the target assembly. Our approach also provides a means of systematically investigating how local modifications to the coordination number through the fusing of adjacent strands affect the nucleation behavior of DNA-brick structures.<sup>24</sup>

The theoretical method used here greatly simplifies the quantitative prediction of nucleation barriers and intermediate structures with widespread applications for controlling the self-assembly of biomolecular or synthetic building blocks. Addressable self-assembly holds great promise for building intricate three-dimensional structures that are likely to require optimization on a case-by-case basis. Because our predictive theory is sensitive to the details of a particular target structure, performing these calculations for nanostructures of experimental interest will enable the precise engineering of assembly properties at the design stage. In order for potential users to perform such experimental protocol design, we provide a user-friendly software package online at <https://github.com/wmjac/pygtsa>.

## ACKNOWLEDGMENTS

This work was carried out with support from the European Research Council (Advanced Grant 227758) and the Engineering and Physical Sciences Research Council Programme Grant EP/I001352/1. W.M.J. acknowledges support from the Gates Cambridge Trust and the National Science Foundation Graduate Research Fellowship under Grant No. DGE-1143678.

## METHODS

### DNA hybridization free energies

We compute the hybridization free energies of complementary 8-nucleotide DNA sequences using established empirical formulae<sup>25,26</sup> assuming salt concentrations of  $[\text{Na}^+] = 1 \text{ mol dm}^{-3}$  and  $[\text{Mg}^{2+}] = 0.08 \text{ mol dm}^{-3}$ . For the calculations with monodisperse bond energies, we use the sequences provided in Ref. 22. The strengths of incidental interactions are estimated based on the longest attractive overlap for each pair of non-complementary sequences. In calculations of the equilibrium yield and free-energy profiles, we report the average thermodynamic properties using 1000 randomly chosen complete sets of DNA sequences. See Sec. S5 for further details.

### Lattice Monte Carlo simulations

Constant-temperature lattice Monte Carlo simulations are carried out using the virtual move Monte Carlo algorithm<sup>16</sup> in order to produce physical dynamics. Rigid particles, each with four distinct patches fixed in a tetrahedral arrangement, are confined to a cubic lattice. A single copy of each required subunit is present in the simulation box with  $62 \times 62 \times 62$  lattice sites. Complete details are given in Ref. 9. For comparison with the results of these simulations, the theoretical calculations reported here assume the same dimensionless monomer concentration,  $\rho = 62^{-3}$ , lattice coordination number,  $q_c = 4$ , and fixed number of dihedral angles,  $q_d = 3$  (see Sec. S1).

<sup>1</sup>Wei B, Dai M, Yin P (2012) Complex shapes self-assembled from single-stranded DNA tiles. *Nature* 485:623–626.

<sup>2</sup>Ke Y, Ong LL, Shih WM, Yin P (2012) Three-dimensional structures self-assembled from DNA bricks. *Science* 338:1177–1183.

<sup>3</sup>Rothmund PW, Winfree E (2000) *The program-size complexity of self-assembled squares* (ACM), pp 459–468.

<sup>4</sup>Zhang Z, Song J, Besenbacher F, Dong M, Gothelf KV (2013) Self-assembly of DNA origami and single-stranded tile structures at room temperature. *Angew Chem Int Ed Engl* 52:9219.

<sup>5</sup>Wei B, et al. (2013) Design space for complex DNA structures. *J Am Chem Soc* 135:18080–18088.

<sup>6</sup>Rothmund PW, Andersen ES (2012) Nanotechnology: The importance of being modular. *Nature* 485:584–585.

<sup>7</sup>Gothelf KV (2012) Lego-like DNA structures. *Science* 338:1159–1160.

<sup>8</sup>Kim AJ, Scarlett R, Biancaniello PL, Sinno T, Crocker JC (2008) Probing interfacial equilibration in microsphere crystals formed by DNA-directed assembly. *Nat Mater* 8:52–55.

<sup>9</sup>Reinhardt A, Frenkel D (2014) Numerical evidence for nucleated self-assembly of DNA brick structures. *Phys Rev Lett* 112:238103.

<sup>10</sup>Jacobs WM, Reinhardt A, Frenkel D (2015) Theoretical prediction of free-energy landscapes for complex self-assembly. *J Chem Phys* 142:021101.

<sup>11</sup>We note that thermodynamically stable partial structures have also been observed in previously reported simulations<sup>9</sup> of DNA-brick structures consisting of approximately 1,000 distinct subunits.

<sup>12</sup>Gibbs JW (1878) On the equilibrium of heterogeneous substances. *Am J Sci* 96:441–458.

<sup>13</sup>Oxtoby DW (1992) Homogeneous nucleation: Theory and experiment. *J Phys Cond Matter* 4:7627.

<sup>14</sup>Sear RP (2007) Nucleation: Theory and applications to protein solutions and colloidal suspensions. *J Phys Cond Matter* 19:033101.

<sup>15</sup>DNA-brick structures have also been assembled at constant temperature by changing the solution conditions during the course of the experiment.<sup>4</sup> For simplicity, we assume that the experimental control parameter is the temperature, but clearly other methods of altering the DNA hybridization free energies during the assembly process may also be suitable.

<sup>16</sup>Whitelam S, Geissler PL (2007) Avoiding unphysical kinetic traps in Monte Carlo simulations of strongly attractive particles. *J Chem Phys* 127:154101.

<sup>17</sup>Incomplete assembly at a constant temperature has also been observed in experiments<sup>27</sup> as well as in our simulations of more complex structures, such as a rectangular slab with a raised checkerboard pattern.

<sup>18</sup>This equilibrium growth pathway is similar to that described in Ref. 28.

<sup>19</sup>Although the coordination number also affects the rotational entropy in lattice-based simulations, altering the rotational entropy in our theoretical method has the same effect as changing the monomer concentration (see Sec. S3) and thus does not affect the shape of the free-energy profile.

<sup>20</sup>Whitelam S, Jack RL (2014) The statistical mechanics of dynamic pathways to self-assembly. *arXiv preprint arXiv:1407.2505*.

<sup>21</sup>Hormoz S, Brenner MP (2011) Design principles for self-assembly with short-range interactions. *Proc Natl Acad Sci USA* 108:5193–5198.

<sup>22</sup>Hedges LO, Mannige RV, Whitelam S (2014) Growth of equilibrium structures built from a large number of distinct component types. *Soft Matter* 10:6404.

<sup>23</sup>Einstein A (1905) Über die von der molekularkinetischen Theorie der Wärme geforderte Bewegung von in ruhenden Flüssigkeiten suspendierten Teilchen. *Ann Phys* 322:549–560.

<sup>24</sup>Li W, Yang Y, Jiang S, Yan H, Liu Y (2014) Controlled nucleation and growth of DNA tile arrays within prescribed DNA origami frames and their dynamics. *J Am Chem Soc* 136:3724–3727.

<sup>25</sup>SantaLucia Jr J, Hicks D (2004) The thermodynamics of DNA structural motifs. *Annu Rev Biophys Biomol Struct* 33:415–440.

<sup>26</sup>Koehler RT, Peyret N (2005) Thermodynamic properties of DNA sequences: Characteristic values for the human genome. *Bioinformatics* 21:3333–3339.

<sup>27</sup>Sobczak JPJ, Martin TG, Gerling T, Dietz H (2012) Rapid folding of DNA into nanoscale shapes at constant temperature. *Science* 338:1458(SI).

<sup>28</sup>Shneidman VA (2003) On the lowest energy nucleation path in a supersaturated lattice gas. *J Stat Phys* 112:293–318.